Measured Forces and Moments on a Delta Wing During Pitch-Up

M. B. Bragg* and M. R. Soltani†
The Ohio State University, Columbus, Ohio

A series of low-speed wind tunnel tests on a 70-deg, sharp, leading-edged delta wing undergoing ramp pitching motion of high amplitude were performed to investigate the aerodynamic forces and moments. Forces and moments were obtained from a six-component internal balance. Large amplitude oscillatory motion was produced by sinusoidally oscillating the model over a range of reduced frequencies. Ramp motion was produced by pitching the model through a half cycle of sinusoidal motion at a root chord Reynolds number of 1.54×10^6. The effect of ramp and oscillatory motions on the forces and moments are almost identical at matched pitch rates. Pitch rate had strong effect on the magnitude of the aerodynamic forces and moments. Upon completion of the model motion, some time is required for the forces and moments to decay to their static values. This convergence of the dynamic values to the static ones was a function of the pitch rate.

Nomenclature

C_D = drag coefficient
C_L = lift coefficient
$C_{L\alpha}$ = variation of lift coefficient with angle of attack (/deg)
C_M = pitching moment coefficient
C_N = normal force coefficient
c = wing root chord, ft
f = frequency, Hz
k = reduced frequency, $\pi fc/U_\infty$
R_e = Reynolds number based on root chord
t = time, s
t^+ = dimensionless time, $2tf$
U_∞ = tunnel speed, ft/s
α = angle of attack, deg
Λ = wing sweep, deg
τ = nondimensional time, tU_∞/c

Introduction

ADVANCED supermaneuverable aircraft operating at a high angle of attack require a substanial amount of nonlinear lift in order to maintain good handling qualities and high performance.[1] There is a growing interest in abandoning angle of attack limitations in low-subsonic flight since most of these poststall flight maneuvers occur at relatively low speed.[2] Such aircraft often utilize highly swept delta wings in order to minimize the aerodynamic drag at supersonic speed and because of their favorable low-speed characteristics.[3]

The flow pattern over these highly swept wings is dominated by a pair of strong vortices above the wing, originating from the sharp leading edge.[4-6] These vortices produce substantial nonlinear lift, called vortex lift, at the moderate angles of attack required during takeoff, landing, and, above all, maneuvers. Some of the present fighter aircraft, such as the F-18 and the F-16, and the next generation of fighters, will employ vortex lift.[7] At high angles of attack, a sudden and dramatic structural change in the vortex, known as vortex breakdown, occurs. Vortex breakdown is characterized by a deceleration of the axial flow in the vortex core.

The aerodynamics of dynamic flight maneuvers are more complicated than the static case because of the unsteady time-dependent flow. The operation of the aircraft may benefit, or be hampered, by this unsteady flow.[8] Large aerodynamic load overshoots can be generated by rapid movements of the aerodynamic surfaces caused by the transient development of separated flow.[9,10] For oscillatory motions, experimental results show that the flow patterns over the wing at any particular angle of attack are different during the upstroke and the downstroke motions.[11-15] Flow lag in the upward motion causes the dynamic stall to occur at higher angles compared to the static case. This is due to the delay in vortex bursting caused by the fast variation of the angle of attack. In the downward motion, the flow remains separated until angles below static stall as a result of the delay in the re-establishment of the leading-edge vortices. These differences in the flow pattern create a hysteresis loop in all forces and moments,[8-15] which are strongly frequency dependent.

Water tunnel results[1] for a delta-wing model of 60 deg sweep angle undergoing ramp pitching motion show a delay in the movement of the vortex bursting position compared to the static case. Also, experimental studies[13-19] using ramp motions show that the nondimensional pitch rate has a strong influence on the position and movement of the vortex breakdown over the wing surface. The pitchup affects the model forces and moments and some time is required after the motion is stopped for steady state values to be reached. Surface pressure measurements over a rectangular wing undergoing ramp motion have shown that the magnitude of the pressure signature increases with increasing the pitch rate.[16,17]

Because of the considerable interest in the maneuverability of combat aircraft in the poststall flight regime, a better understanding of the flow mechanisms and the associated forces and moments during a ramp pitchup is imperative. While research is continuing in this area,[8-10,13-18] the effect of a ramp-pitch maneuver on the delta-wing forces and moments is not completely understood. The specific focus in this paper is to study the effect of pitch rate and amplitude on the aerodynamic forces and moments generated by a 70-deg, sharp, leading-edged delta-wing model. Longitudinal forces and moments are studied as the delta wing experiences a sinusoidal ramp in pitch.

Experimental Procedure

The experiments were conducted in the subsonic wind tunnel of the Ohio State University's Aeronautical and Astronau-

Received May 10, 1989; revision received Sept. 6, 1989.

*Associate Professor, Department of Aeronautical and Astronautical Engineering; currently at the University of Illinois, Urbana, Illinois. Senior Member AIAA.

†Graduate Research Assistant, Department of Aeronautical and Astronautical Engineering. Member AIAA.

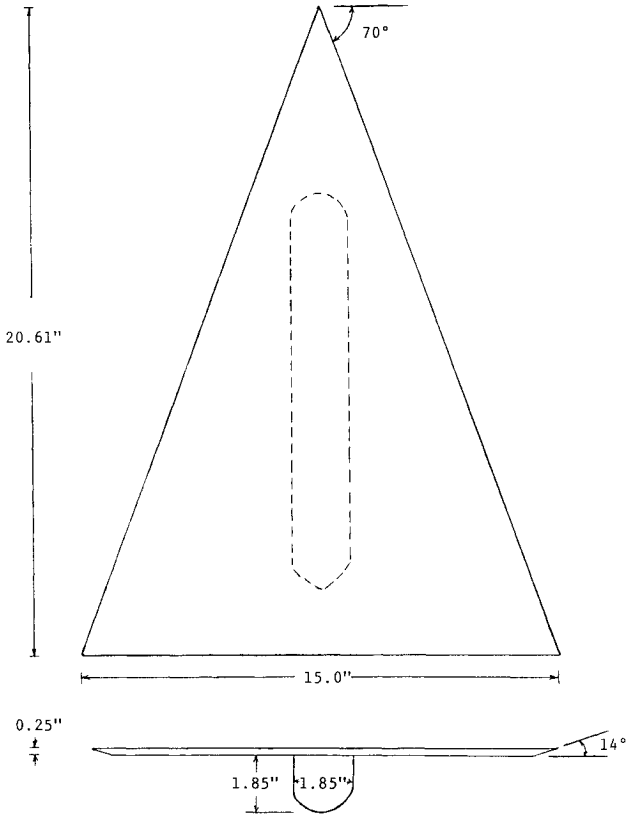

Fig. 1 Delta wing model (dimensions in inches).

tical Research Laboratory. The tunnel test section is approximately 5 ft wide, 3 ft high, 8 ft long, and operates at speeds from 0 to 200 ft/s at a Reynolds number of up to 1.3×10^6/ft. The tunnel is of open return type and uses four large antiturbulence screens and honeycomb to attain a low turbulent intensity.

Model

The model was a simple flat-plate delta wing of a 70-deg leading-edge sweep, a 20.61-in. root chord, and a 15-in. span at the trailing edge. The wing was constructed of 1/4-in. thick aluminum. The leading and trailing edges were sharpened by tapering up from the lower surface at 14 deg. A pod large enough to house the balance and necessary hardware was attached under the wing. A drawing of the model used in this investigation is shown in Fig. 1.

Oscillation System

The oscillation system of Ref. 11 was modified for use in the study. The system uses a belt and pulley arrangement to drive a cam designed to produce a continuous sinusoidal oscillation of the form

$$\alpha(t) = 55 - 27.5[1 + \cos(2\pi ft)]$$

The system was modified to produce sinusoidal ramp motions by installing a computer-controlled solenoid clutch in the belt reduction system. This allows the cam to be rapidly connected/disconnected from the motor drive. Thus sinusoidal ramps can be created at varying frequency using segments of the sinusoidal motion.

Figure 2 shows the model angle of attack vs time for the various ramp motions used in this study. The dashed line shows a portion of the continuous sinusoidal motion. In the top diagram, ramp motions starting at 0 deg angle of attack are shown. In each case the clutch is engaged and the model angle of attack increases along the upstroke of the sinusoidal

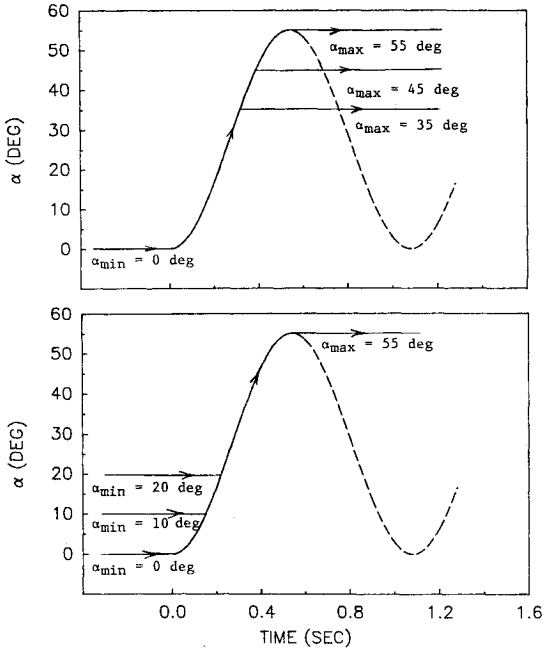

Fig. 2 Ramp and sinusoidal model motions used in this study ($f = 0.926$ Hz).

oscillation until the clutch is disengaged when the desired maximum amplitude of 35, 45, or 55 deg is reached. In the lower plot, sinusoidal ramps starting at 0, 10, and 20 deg angle of attack are shown. The model pitch rate is varied by changing the frequency of rotation of the sinusoidal cam.

For a linear ramp[16,17] the pitch rate $\dot{\alpha}$ is constant with respect to time and a nondimensional pitch rate $\alpha^+ = \dot{\alpha}c/U_\infty$ is used.[16,17] Here it is not convenient to use the nondimensional pitch rate α^+ since $\dot{\alpha}$ is not constant but varies sinusoidally. The ramp motions used in this paper are all derived from sections of a continuous oscillatory motion of frequency f. Therefore, the usual reduced frequency $k = \pi fc/U_\infty$ will be used here to describe the ramp motion and will be referred to in this paper as the nondimensional pitch rate.

The model was oscillated about its 57% root-chord location and 3 in. below the chord line. The desire to locate the balance pod on the wing to minimize its aerodynamic effect and to oscillate the model near the balance moment center determined this oscillation location.

Force Measurement

Force measurements were made using a six-component internal strain gauge balance. There are two types of forces and moments which must be subtracted out of the data as tares. The first are the gravitational loads due to the model and balance weight which are functions of the angle of attack. The second are the inertial forces and moments produced by the moments of inertia of the model and balance in dynamic motion. Both of these forces and moments have been measured and subtracted from the wind-on data.[11]

Data Acquisition and Reduction

The data acquisition system was developed specifically for this investigation. Data were taken and reduced on a personal computer. The computer is equipped with a 12-bit, 16-channel analog to digital board. For this experiment 10 channels of data were measured: 6 for balance data, 1 for potentiometer input, 2 for tunnel speed, and 1 hot-film channel.

The sample rate used in acquiring these data varied based on the reduced frequency but was nominally 100 Hz per channel. Data were taken and reduced to engineering units on the personal computer, then uploaded to the main laboratory computer. The data were then digitally filtered to provide low-pass

filtering at approximately 10 Hz, well below the model support natural frequency.

Aerodynamic forces and moments were measured at the balance moment center and have been transferred to the 25% wing-root chord station. All moments were nondimensionalized with respect to two-thirds wing root chord. Longitudinal forces and moments are in the wind axis system.[20]

Blockage corrections at a small angle of attack were determined by the method of Ref. 20 and were found to be small. In addition Ref. 21 suggests that blockage ratios of less than 7% can usually be considered negligible. The blockage ratio for this investigation was 6%. Thus no correction has been applied to the data.

Results and Discussion

The purpose of the present investigation was to examine the effect of pitch rate and initial and final angle of attack on the forces and moments on a delta wing undergoing a ramp motion in pitch. The experiments were performed on a 70-deg sharp, leading-edge delta wing and included static and forced sinusoidal oscillation at various reduced frequencies. Detailed analysis of the static results along with the continuous oscillation data at various reduced frequencies and Reynolds number effect are presented in Refs. 11 and 12. Further information and discussion of the data can be found in Ref. 13.

Dynamic Pitch-Up

The influence of the nondimensional pitch rate on the forced unsteady flow over the 70 deg, sharp leading-edge model was investigated by pitching the model at different rates from 0, 10, and 20 deg to 55, 45, and 35 deg angles of attack. Although many different motion profiles are possible, only a single sinusoidal ramp motion was examined. Data for three different nondimensional pitch rates are presented in this paper, $k = 0.0152$, 0.0357, and 0.0463. All runs were made at a Reynolds number of 1.54×10^6 based on the root chord.

In presenting the data, angular velocities and time have been nondimensionalized. Two nondimensional times are used. Time nondimensionalized by convective time is referred to as τ. It is also convenient to use a nondimensional time, $t^+ = 2$ ft. This allows data taken at different pitch rates to be compared at the same angle of attack. This type of nondimensionalization is also used in Ref. 19.

The variation of normal force coefficient with the nondimensional pitch rate is plotted vs τ, time nondimensionalized by convective time, for the 0–55-deg ramp in Fig. 3. The static value of $C_{N\max}$ at 55 deg is also shown as a baseline. The effect of nondimensional pitch rate on the character of the normal force coefficient is clear. The maximum value of the normal force coefficient increases with increasing the pitch rate. This agrees with the previous pressure measurement results of Ref. 16 and 17 where increasing the pitch rate lowers the pressure signature and hence produces higher forces and moments. Comparison of the static $C_{N\max}$ with the maximum ramp values shows a substantial increase in the maximum normal force overshoot due to the pitch rate. Also, from Fig. 3 note that as the pitch rate increases, maximum normal force occurs at higher angles of attack, a phenomenon caused by the delay in dynamic stall because of the fast variation of the angle of attack.

The lift performance of the delta wing at the nondimensional pitch rates is shown in Fig. 4. Included in this figure is the static value of $C_{L\max}$ and C_L at 55 deg angle of attack. Note that although $C_{L\max}$ for the ramp motion is substantially higher than the static $C_{L\max}$, it remains constant with further increasing pitch rate. This is an interesting result and contradicts the usual perception of force overshoots increasing with frequency or pitch rate. This has also been noticed in earlier three-dimensional oscillation data[10-12] and in two-dimensional unsteady data.[18]

To resolve lift from the normal and axial force measurements

$$C_L = C_N \cos(\alpha) - C_A \sin(\alpha)$$

For the delta-wing model used here, axial forces can be generated only by shear, pressure differences between leading and trailing edges or on the balance pod. The axial force is therefore small compared to the normal force at non-zero angles of attack. While the lift data presented in this report contain the axial force contribution, only the dominant C_N term is considered here

$$C_L \simeq C_N \cos(\alpha)$$

Maximum lift and normal force coefficients and the angle of attack at which each occur are found in Figs. 5 and 6 as a

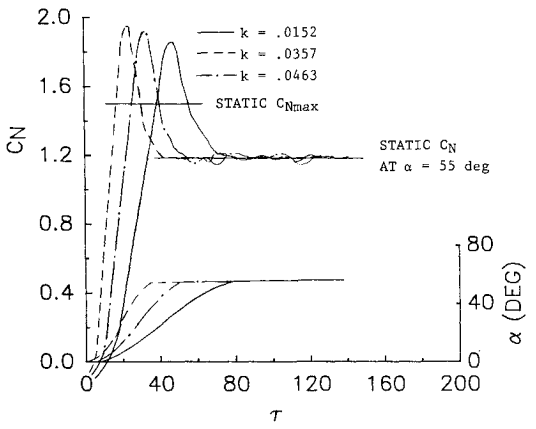

Fig. 3 Effect of nondimensional pitch rate on normal force coefficient.

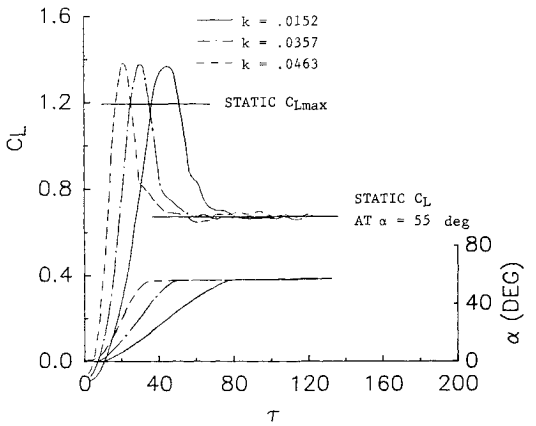

Fig. 4 Effect of nondimensional pitch rate on lift coefficient.

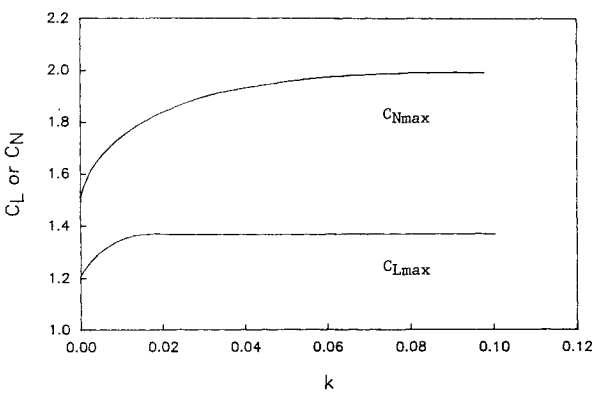

Fig. 5 Maximum normal force and lift coefficient vs nondimensional pitch rate.

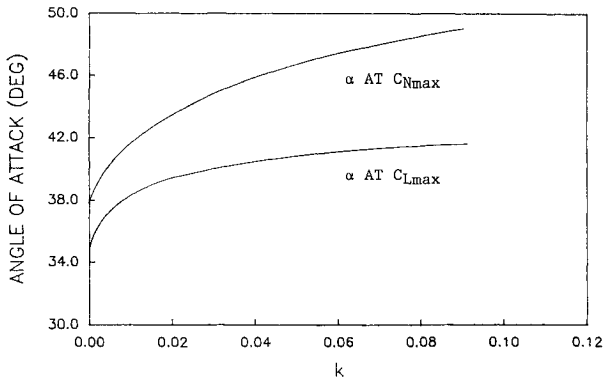

Fig. 6 Angle of attack for maximum normal force and lift coefficient vs nondimensional pitch rate.

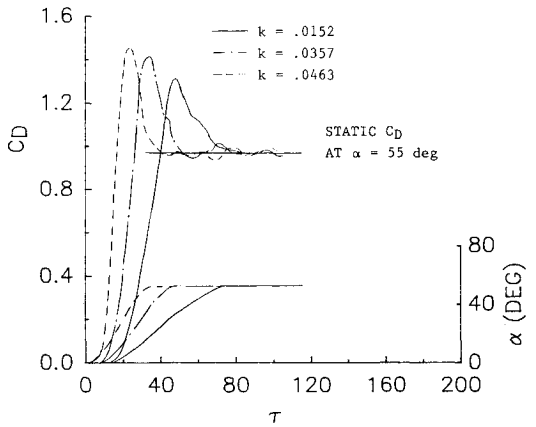

Fig. 7 Effect of nondimensional pitch rate on drag coefficient.

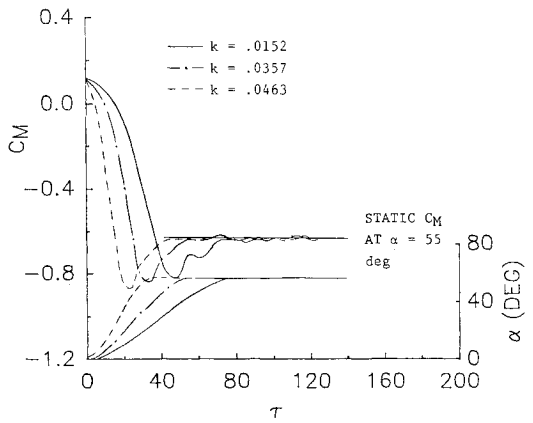

Fig. 8 Effect of nondimensional pitch rate on pitching moment coefficient.

function of nondimensional pitch rate. The $C_{N\max}$ is seen to increase with pitch rate, but the angle of attack at which it is reached also increases. Beyond approximately $k=0.04$, the rate of rise of $C_{N\max}$ decreases significantly (see Fig. 5). From Fig. 6, it is seen that α at $C_{N\max}$ rises rapidly beyond $k=0.04$. These phenomena indicate that beyond a certain reduced frequency, the flow lag reduces. This agrees with the previous low visualization results of Ref. 10. Since $C_L \simeq C_N \cos(\alpha)$, the relationship between C_L and C_N depends strongly on α, and $C_{L\max}$ occurs at a lower angle of attack than $C_{N\max}$. For example, at $k=0.0357$ $C_{N\max}$ occurs at about 44 deg angle of attack and $C_{L\max}$ occurs at about 40 deg. The $C_{L\max}$ remains almost constant with increasing frequency after an initial substantial rise at low k. The $C_{N\max}$ rises sharply at low k but continues to increase even at a nondimensional pitch rate of 0.088, the

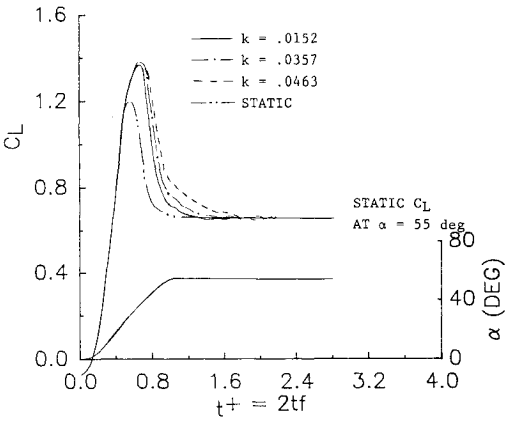

Fig. 9 Lift coefficient vs dimensionless time during a pitch-up.

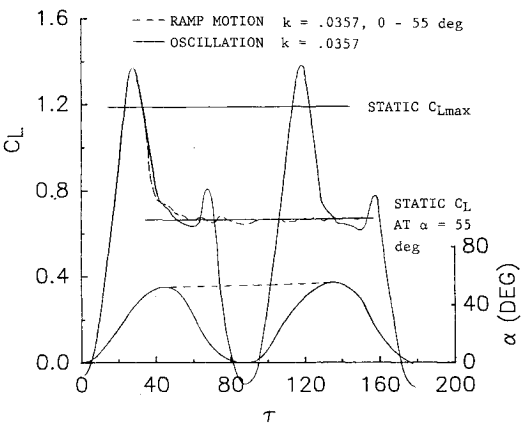

Fig. 10 Comparison of continuous and ramp data vs dimensionless time.

highest value tested. The combination of higher $C_{N\max}$ with increasing k, but at higher α, almost cancel each other to prevent much change in $C_{L\max}$.

The drag force can be expressed approximately as

$$C_D \simeq C_N \sin(\alpha)$$

when at large α, where the axial force is small compared to the normal force. Here, since C_D goes like $\sin(\alpha)$, this contribution increases with increasing α. In Fig. 7, the drag coefficient data are shown corresponding to Figs. 4 and 5. Here $C_{D\max}$ occurs at approximately the same angle as $C_{N\max}$ and therefore trends very closely with $C_{N\max}$ when pitch rate is varied.

Pitching moment data for the model are shown in Fig. 8. In addition, the static value of C_M at 55 deg angle of attack is shown. At 0 deg angle of attack, the presence of the slight nose-up pitching moment is produced by the negative normal force (see Fig. 3) due to the balance pod and taper of the lower surface leading edge. By increasing the angle of attack, a negative pitching moment is produced, which indicates that the center of pressure moves aft of the reference point (one-quarter wing root chord). Note when comparing Figs. 3 and 8 that C_M reaches its maximum negative value at approximately the same nondimensional time that C_N reaches $C_{N\max}$. Further increase in the incidence is followed by a substantial reduction in the nose-down pitching moment. This is caused by the forward progression of the vortex burst point on the wing surface. As the vortex breakdown moves onto the wing, the pressure on the upper surface aft of the bursting increases considerably reducing the normal force on the rear portion of the wing which lessens the nose-down pitching moment.[6] The influence of the pitch rate on the maximum pitching-moment

overshoot is apparent. As the pitching maneuver stops (55 deg angle of attack), the curves continue moving toward the static C_M at a rate which varies with the pitch rate.

Figure 9 shows the resulting lift coefficient vs nondimensional time t^+ defined as $t^+ = 2tf$ for the 0–55-deg ramp at various pitch rates. Also shown in the same figure are the corresponding static data (at matched angle of attack) and the variation of angle of attack. Note that the angle of attack is a function of t^+, and therefore plotting the data in this way allows the comparison of data at identical angles of attack when the data were taken at different pitch rates. Substantial increases in the lift coefficient for the ramp case are seen when compared to the static data. For the static case, as previously mentioned, maximum lift coefficient is about 1.2 occurring at an incidence of about 35 deg. For the ramp data, the maximum lift coefficient is approximately 1.37 and occurs at an incidence of 40 deg (see Fig. 4). As previously indicated, the delay in dynamic stall angle and the overshoot in the maximum lift coefficient is caused by the vortex bursting crossing the wing trailing edge at a higher angle of attack during the pitch-up. Note that on the upstroke, before $C_{L\max}$, the lift at constant angle of attack (i.e, t^+) is almost independent of pitch rate. However, once the angle of attack reaches the maximum lift angle, the lift decay is a function of pitch rate with the lift at higher pitch rates decaying to the static value more slowly. These results compare with the flow visualization findings of Ref. 19 using the same model geometry and ramp pitching motion.

Figure 10 compares the resulting lift coefficient of the 70-deg, sharp leading-edge model for the ramp and oscillation motion at a reduced frequency of 0.0357. Static data for both $C_{L\max}$ and the lift coefficient at 55 deg angle of attack are shown. It is seen that the lift coefficient for the ramp motion follows that of the continuous oscillation almost exactly until 55 deg angle of attack is reached. Also note that for the second oscillation shown, the lift is practically identical to the first oscillation. In fact, the several cycles of data which were taken are the same. Therefore, even after several cycles, the sinusoidal ramp and the continuous oscillation data are essentially identical in the upstroke, at least for the reduced frequencies and angles of attack considered here. See Refs. 11–13 for an analysis of the variation of the aerodynamic forces and moments with angle of attack in continuous sinusoidal oscillation.

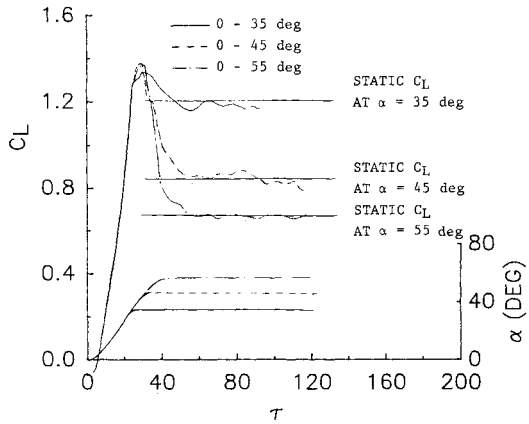

Fig. 11 Effect of ramp maximum angle of attack on lift coefficient.

Up to now, the influence of the pitch rate on the character of the aerodynamic forces and moments of the delta wing model when it was ramped 0 to 55 deg angle of attack was investigated. In the following section, variation of the lift and drag coefficient vs τ for the ramp motion to 35, 45, and 55 deg angle of attack and at a constant pitch rate will be examined.

Figure 11 shows the variation of the lift coefficient vs τ at a constant nondimensional pitch rate of 0.0357. Static data for 35, 45, and 55 deg angle of attack are also shown for comparison. Maximum lift overshoot in the ramp data caused by the convective time lag of the adjusting flowfield is apparent. From Fig. 11, it is seen that $C_{L\max}$ for the 0–45 and 0–55 deg ramp motions occur at an incidence of about 41 deg for this particular pitch rate. For the 0–35 deg pitch-up, $C_{L\max}$ is obtained after the model has reached 35 deg angle of attack. However, as a result of the vortex breakdown progression over the wing, they rapidly drop to their static values which are far below the dynamic $C_{L\max}$. The nondimensional time required for the model to return to the static C_L, once the dynamic $C_{L\max}$ has been reached, increases as the maximum ramp angle increases.

Figure 12 shows the corresponding drag force data of the model for both static and ramp motion. Also shown in the figure are the static data for 35, 45, and 55 deg angle of attack. Again a much higher drag is evident when compared to the maximum drag coefficient of the static case. The overshoot in the maximum drag force drops to the static value when the motion is ceased. This reduction coincides with the drop in the maximum normal force coefficient caused by the vortex burst movement on the wing surface. From Fig. 12, for the ramp motion of 0–35 deg angle of attack, the drag coefficient overshoot was small compared to the 45 and 55 deg ramps. Interestingly, the same trend is observed in the normal force and pitching moment data.

The model lift coefficient vs τ at three different ramp motions of 0, 10, and 20–55 deg angle of attack for a constant nondimensional pitch rate of 0.0355 is shown in Fig. 13. Static data at 55 deg angle of attack are also shown on the plot. No significant change in the character of the lift data for the preceding motions is observed. Data for other forces and moments also show no significant effect. It is noted that at both

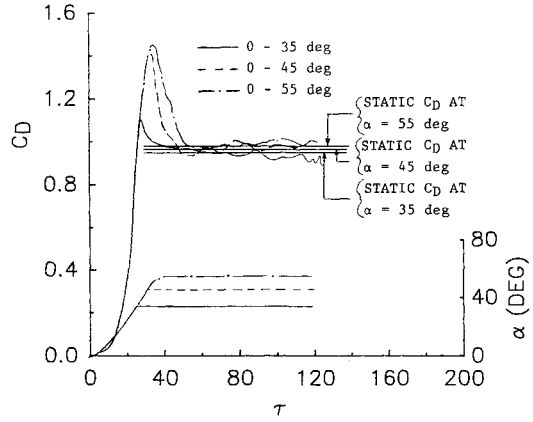

Fig. 12. Effect of ramp maximum angle of attack on drag coefficient.

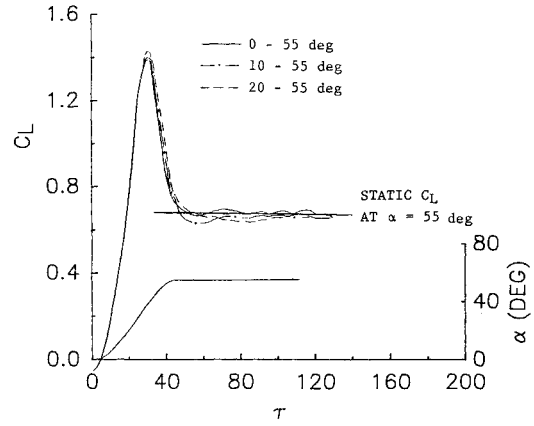

Fig. 13 Effect of starting ramp angle of attack on lift coefficient.

$\alpha = 10$ and 20 deg, the vortex burst point has not yet reached the wing trailing edge. For the 70-deg-sweep, delta-wing model in steady pitch-pause motion, the vortex burst point reaches the trailing edge at an angle of attack of about 27 deg.[12] For starting angles above 27 deg angle of attack, the burst point will be on the wing, and the results may be different. Unfortunately, these data are not available. The preceding cases at other nondimensional pitch rates followed the same trend, and therefore will not be presented.

Conclusions

The major objective of this experiment was to investigate the forces and moments on a 70-deg sweep, sharp, leading-edged, delta-wing model driven with a sinusoidal ramp pitch motion beyond the angle of attack for static stall. Pitch rate and the initial and final ramp angle of attack were studied. From the data the following conclusions can be drawn.

1) All aerodynamic forces and moments are found to be affected by the magnitude of the pitch rate. Dynamic stall for all of the reduced frequencies tested occurred at higher angles of incidence than the corresponding static stall. This is a result of the flow lag in the vortex burst progression over the wing surface. However, $C_{L\max}$ was not strongly affected by the pitch rate after an initial increase at low pitch rate.

2) The influence of the nondimensional pitch rate on the transient normal force seems to decrease beyond a certain reduced frequency. The angle at which maximum normal force occurs increases with increasing pitch rate.

3) The forces due to the ramp motion closely followed that of the oscillatory case during pitch up. However, when the pitch-up motion was terminated, the decay of the aerodynamic forces was influenced by the pitch rate.

4) Initiating the ramp motion at 0, 10, or 20 deg angle of attack for the pitchup to 55 deg had little effect on the measured forces and moments.

5) Terminating the ramp at 45 or 55 deg angle of attack produced almost identical results—although slightly larger overshoots for the 55-deg case. The ramp to 35 deg produced significantly lower overshoots. The time to return to the static value increases as the maximum ramp angle increases.

Acknowledgments

This work was supported in part by Grant NAG-1-641 from NASA Langley Research Center. The authors would like to thank Jay Brandon of NASA Langley for his guidance in performing this experiment.

References

[1]Wolffelt, K. W., "Investigation of the Movements of Vortex Burst Position with Dynamically Changing Angle of Attack for a Schematic Delta Wing in a Water Tunnel With Correlation to Similar Studies in a Wind Tunnel," AGARD-CP-413, 1986, pp. 27-1–27-8.

[2]John, H., and Kraus, W., "High Angle of Attack Characteristics of Different Fighter Configurations," AGARD-CP-247, 1978, pp. 2-1—2-15.

[3]Verhaagen, N. G. "Some Low-Speed Wind Tunnel Experiments on a Sharp-Edged Delta Wing of Aspect Ratio 1, With and Without Yaw," Delfta University of Technology, Delft, The Netherlands, Rept. LR-283, Aug. 1979.

[4]Elle, B. J., and Jones, J. P., "A Note on The Vorticity Distribution on The Surface of Slender Delta Wings With Leading Edge Separation," *Journal of the Royal Aeronautical Society*, Vol. 65, March 1961, pp. 195–198.

[5]Wentz, W. H., "Wind Tunnel Investigations of Vortex Breakdown on Slender Sharp-Edged Wings," Ph. D. Dissertation, University of Kansas, Lawrence, KS, 1968.

[6]Hummel, D., and Srinivasan, P. S., "Vortex Breakdown Effects on the Low-Speed Aerodynamic Characteristics of Slender Delta Wings in Symmetrical Flow," *Journal of the Royal Aeronautical Society*, Vol. 71, April 1967, pp. 319–322.

[7]Erikson, G. E. et al., "Experimental Investigation of the F/A-18 Vortex Flows at Subsonic Speeds," AIAA Paper 89-2222, 1989.

[8]Gad-el-Hak, M., and Ho, C.-M., "The Pitching Delta Wing," *AIAA Journal*, Vol. 23, No. 11, Nov. 1985, pp. 1160–1665.

[9]Mabey, D. G., "On the Prospects for Increasing Dynamic Lift," *The Aeronautical Journal of the Royal Aeronautical Society*, Vol. 92, No. 913, March 1988, pp. 95–106.

[10]Jarrah, M.-A. M., "Low-Speed Wind-Tunnel Investigation of Flow About Delta Wings, Oscillating in Pitch to Very High Angle of Attack," AIAA Paper 89-0295, Jan. 1989.

[11]Soltani, M. R., Bragg, M. B., and Brandon, J. M., "Experimental Measurements on an Oscillating 70-Degree Delta Wing In Subsonic Flow," AIAA Paper 88-2576, June 1988.

[12]Soltani, M. R., Bragg, M. B., and Brandon, J. M., "Measurements on an Oscillating 70-Degree Delta Wing In Subsonic Flow," *Journal of Aircraft*, Vol. 27, No. 3, 1990 pp. 211–217.

[13]Bragg, M. B., and Soltani, M. R., "An Experimental Study of the Effect of Asymmetrical Vortex on a Pitching Delta Wing," AIAA Paper 88-4334, Aug. 1988.

[14]Cunningham, A. M., Jr., "Unsteady Low-Speed Wind Tunnel Test of a Strake Delta Wing, Oscillating in Pitch," Air Force Wright Aeronautical Lab., Wright-Patterson AFB, OH, TR-87-3098, Parts I and V, April 1988.

[15]LeMay, S. P., Batill, S. M., and Nelson, R. C., "Leading Edge Vortex Dynamics on a Pitching Delta Wing," University of Notre Dame, Notre Dame, IN, Nag-1-727, April 1988.

[16]Robinson, M. C., and Wissler, J. B., "Pitch Rate and Reynolds Number Effects on a Pitching Rectangular Wing," AIAA Paper 88-2577, June 1988.

[17]Walker, J. M., Robinson, M. C., and Seiler, F. J., "Impingement of Orthogonal Unsteady Vortex Structures on Trailing Aerodynamic Surfaces," AIAA Paper 88-2580, June 1988.

[18]Francis, M. S., and Keesee, J. E., "Airfoil Dynamic Stall Performance With Large-Amplitude Motions," *AIAA Journal*, Vol. 23, No. 11, Nov. 1985, pp. 1653–1659.

[19]Thompson, S., Batill, S., and Nelson, R., "The Separated Flow Field on a Slender Delta Wing Undergoing Transient Pitching Motions," AIAA Paper 89-0194, Jan. 1989.

[20]Rae, W. H., and Pope, A., *Low-Speed Wind Tunnel Testing*, 2nd ed., Wiley, New York, 1984.

[21]Pass, C. Q., "A Wake Blockage Correction Method for Small Subsonic Wind-Tunnnels," AIAA Paper 87-0294, Jan. 1987.